

Goos-Hänchen-like shifts for Dirac fermions in monolayer graphene barrier

Xi Chen^{1,2,*}, Jia-Wei Tao¹, and Yue Ban²

¹ Department of Physics, Shanghai University, 200444 Shanghai, China and

² Departamento de Química-Física, UPV-EHU, Apdo 644, 48080 Bilbao, Spain

(Dated: October 30, 2018)

We investigate the Goos-Hänchen-like shifts for Dirac fermions in transmission through a monolayer graphene barrier. The lateral shifts, as the functions of the barrier's width and the incidence angle, can be negative and positive in Klein tunneling and classical motion, respectively. Due to their relations to the transmission gap, the lateral shifts can be enhanced by the transmission resonances when the incidence angle is less than the critical angle for total reflection, while their magnitudes become only the order of Fermi wavelength when the incidence angle is larger than the critical angle. These tunable beam shifts can also be modulated by the height of potential barrier and the induced gap, which gives rise to the applications in graphene-based devices.

PACS numbers: 73.23.Ad, 42.25.Gy, 72.90.+y, 73.50.-h

I. INTRODUCTION

Monolayer graphene has attracted much attention^{1,2} since the graphitic sheet of one-atom thickness has been experimentally realized by A. K. Geim *et al.* in 2004³. The valence electron dynamics in such a truly two-dimensional (2D) material is governed by a massless Dirac equation. Thus graphene has many unique electronic and transport properties^{1,2}, including Klein tunneling⁴. Recently, further investigations show that a method to produce a finite bandgap in graphene sheets by epitaxially on proper substrate⁵ has been proposed, and the Dirac fermions in gapped graphene are described by 2D massive Dirac equations. The induced gap at the Dirac point is significant to control the transport of the carriers and integrating graphene into the semiconductor technology.

Motivated by these progress, the transport of massive or massless Dirac fermions in graphene opens a way to design various graphene-based electron devices in term of the electron optics behaviors⁶⁻¹¹, such as focusing⁶, collimation⁷, Bragg reflection⁹, and Goos-Hänchen effect (GH)^{10,11}. In particular, Zhao and Yelin¹⁰ have shown that, based on the electronic counterpart to the trapped rainbow effect in optics¹², the interplay GH effect and negative refraction⁶ in graphene leads to the coherent graphene devices, such as movable mirrors, buffers and memories. Beenakker *et al.*¹¹ have further found that the GH effect at a *n-p* interface in graphene doubles the degeneracy of the lowest propagating mode, which can be observed as a stepwise increase by $8e^2/h$ of the conductance with increasing channel width.

In this paper, we will investigate the negative and positive lateral shifts for Dirac fermions in transmission through a 2D monolayer graphene barrier, based on the tunable transmission gap¹³. Generally, the magnitude of GH shift for total reflection in graphene is in the order of Fermi wavelength. However, the lateral shifts discussed here are similar to but different from the conventional GH shift, because they do result from the beam width of Dirac fermions, and can be enhanced by the transmis-

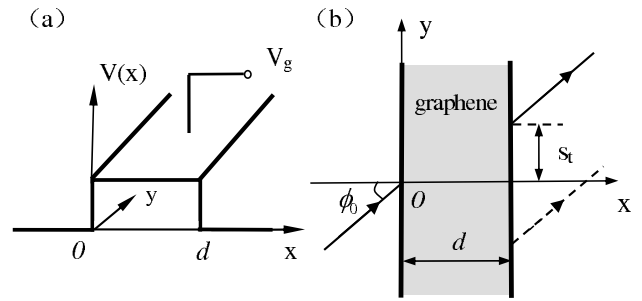


FIG. 1. (a) Schematic diagram for two-dimensional monolayer graphene barrier. (b) Negative and positive lateral shifts of Dirac fermions in transmission.

sion resonances. As a matter of fact, the lateral shifts in transmission have nothing to do with the evanescent wave, thus we term them as Goos-Hänchen-like (GHL) shift, which can be considered as an electronic analog of the lateral shifts in the optics¹⁴ and atom optics¹⁵. More interestingly, not only large positive but also large negative GHL shifts can occur in transmitted beam through the graphene barrier. The negative shift behaves like the phenomena of negative refraction in graphene⁶. In addition, we will also discuss the effect of the induced gap on the GHL shifts in the gapped graphene barrier. All these tunable beam shifts in the monolayer graphene barrier can be applied in the design of graphene-based devices, such as electron wave switch, wave vector or energy filters and splitter.

II. THEORETICAL MODEL

Consider the massless Dirac fermions with Fermi energy E at angle ϕ_0 with respect to the x axis incident from zero-gap graphene upon a 2D gapped graphene barrier of height V_0 in which the electron acquires a finite mass of Δ/v_f^2 , as shown in Fig. 1, where the tunable potential barrier is formed by a bipolar junction (*p-n-p*) within a single-layer graphene sheet with top gate volt-

age V_g ¹⁶, V_0 and d are the height and width of potential barrier, respectively. Since graphene is a 2D zero-gap semiconductor with the linear dispersion relation, $E = \hbar k_f v_f$, the massless electrons are formally described by the Dirac-like hamiltonian⁴, $\hat{H}_0 = -i\hbar v_f \sigma \nabla$, where $v_f \approx 10^6 m \cdot s^{-1}$ is the Fermi velocity, k_f is the Fermi wave vector ($\lambda = 2\pi/k_f$ is Fermi wavelength), and $\sigma = (\sigma_x, \sigma_y)$ are the Pauli matrices. The wave functions of the plane wave components for the incident and reflected regions are assumed to be

$$\Psi_I = \begin{pmatrix} 1 \\ s e^{i\phi} \end{pmatrix} e^{i(k_x x + k_y y)} + r \begin{pmatrix} 1 \\ -s e^{-i\phi} \end{pmatrix} e^{i(-k_x x + k_y y)}, \quad (1)$$

so the corresponding wave function in the transmitted region can be expressed by

$$\Psi_{III} = t \begin{pmatrix} 1 \\ s e^{i\phi} \end{pmatrix} e^{i(k_x x + k_y y)}, \quad (2)$$

where $s = \text{sgn}(E)$, $k_x = k_f \cos \phi$ and $k_y = k_f \sin \phi$ are the perpendicular and parallel wave vector components outside the barrier, ϕ is the incidence angle of the plane wave component under consideration. For the general case of the gapped graphene barrier, the Hamiltonian of massive Dirac fermions can be written down as $\hat{H}_1 = -i\hbar v_f \sigma \nabla + \Delta \sigma_z$, where Δ is equal to the half of the induced gap in graphene spectrum and positive (negative) sign corresponds to the K (K') point, thus the wave functions in the barrier region have the following form:

$$\Psi_{II} = \begin{pmatrix} \alpha \\ s' \beta e^{i\theta} \end{pmatrix} e^{i(q_x x + k_y y)} + \begin{pmatrix} \alpha \\ -s' \beta e^{-i\theta} \end{pmatrix} e^{i(-q_x x + k_y y)}, \quad (3)$$

where $s' = \text{sgn}(E - V_0)$, $k'_f = \sqrt{(V_0 - E)^2 - \Delta^2} / \hbar v_f$, $q_x = (k'_f{}^2 - k_y^2)^{1/2}$, $\theta = \arctan(k_y / q_x)$, α and β are defined by

$$\alpha = \sqrt{1 + \frac{s' \Delta}{\sqrt{\Delta^2 + k_f'^2}}}, \quad \text{and} \quad \beta = \sqrt{1 - \frac{s' \Delta}{\sqrt{\Delta^2 + k_f'^2}}}.$$

Accordingly, the critical angle ϕ_c for total reflection can be defined by

$$\phi_c = \arcsin \left[\frac{(V_0 - E)^2 - \Delta^2}{E^2} \right]^{1/2}, \quad (4)$$

so that when $\phi > \phi_c$, the wave function in the propagating case becomes evanescent wave by replacing q_x with $i\kappa$, where $\kappa = (k_y^2 - k_f'^2)^{1/2}$. According to the boundary conditions, the transmission coefficient $t \equiv e^{i\varphi} / f$ is determined by

$$t = \frac{1}{\cos(q_x d) - i(ss' \chi \sec \phi \sec \theta + \tan \phi \tan \theta) \sin(q_x d)}, \quad (5)$$

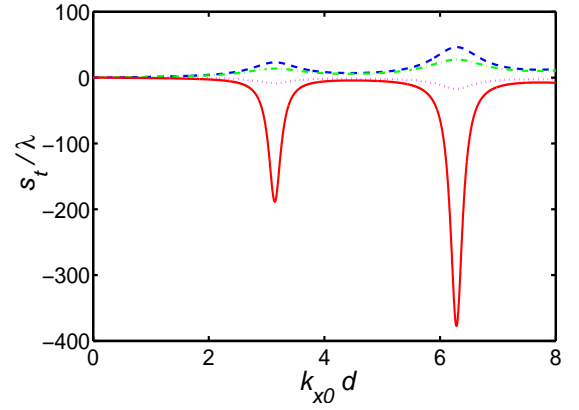


FIG. 2. (Color online) Dependence of GHL shifts in the propagating case on the barrier's width d , where $\phi_0 = 25^\circ$, $V_0 = 120 \text{ meV}$, d is re-scaled to $k_{x0} d$, $E = 80 \text{ meV}$, $\Delta = 20 \text{ meV}$ (solid line), $E = 220 \text{ meV}$, $\Delta = 20 \text{ meV}$ (dashed line), $E = 80 \text{ meV}$, $\Delta = 0 \text{ meV}$ (dotted line), and $E = 220 \text{ meV}$, $\Delta = 0 \text{ meV}$ (dot-dashed line).

where $\chi = \sqrt{\Delta^2 + k_f'^2} / k_f'$ and the phase shift φ is obtained by

$$\varphi = \arctan \left[\frac{\sin \theta \sin \phi + ss' \chi}{\cos \theta \cos \phi} \tan(q_x d) \right]. \quad (6)$$

From the above expression, it is clear that in the limit $\Delta \rightarrow 0$, we get $\chi = 1$ and thus one can obtain the same expression for electronic transmission probability $T = 1/f^2$ corresponding to the massless Dirac fermions¹³.

For a well-collimated beam with the central angle ϕ_0 of incidence, the GHL shift can be defined, according to the stationary phase method^{10,17}, as

$$s_t = -\frac{\partial \varphi}{\partial k_{y0}}, \quad (7)$$

where the subscript 0 in this paper denotes the values taken at $\phi = \phi_0$. The most intriguing behavior in propagating case is found for Klein tunneling, $E < V_0$, where the GHL shifts can be negative, and also be enhanced by the transmission resonances, whereas the lateral shifts for classical motion, $E > V_0$, are always large and positive. Examples of their dependence on the barrier's width at different induced gaps Δ are plotted in Fig. 2, where $E = 80 \text{ meV}$, $V_0 = 120 \text{ meV}$, $\phi = 25^\circ$ is less than the critical angle defined by Eq. (4), solid and dotted lines correspond to Klein tunneling $E = 80 \text{ meV} < V_0$, and dashed and dot-dashed ones correspond to classical motion $E = 220 \text{ meV} > V_0$. On the contrary, when the incident angle ϕ_0 is larger than the critical angle ϕ_c , the lateral shifts become in the order of Fermi wavelength due to the evanescent wave, which is similar to those in total reflection at a single graphene interface^{10,11}. Instead of

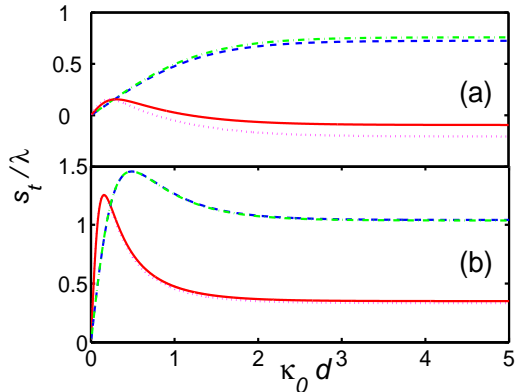


FIG. 3. (Color online) Dependence of GHL shifts in the evanescent case on the barrier's width d , where (a) $\phi_0 = 35^\circ$ and (b) $\phi_0 = 75^\circ$, d is re-scaled to $\kappa_0 d$, $E = 80 \text{ meV}$, $\Delta = 20 \text{ meV}$ (solid line), $E = 220 \text{ meV}$, $\Delta = 20 \text{ meV}$ (dashed line), $E = 80 \text{ meV}$, $\Delta = 0 \text{ meV}$ (dotted line), and $E = 220 \text{ meV}$, $\Delta = 0 \text{ meV}$ (dot-dashed line).

the enhancement by the transmission resonances shown in Fig. 2, Fig. 3 illustrates that the GHL shifts for Klein tunneling and classical motion saturate respectively to negative and positive constants with increasing the barrier's width in the evanescent case, where (a) $\phi_0 = 35^\circ$ and (b) 75° , d is re-scaled to $\kappa_0 d$, the other parameters are the same as in Fig. 2.

III. DISCUSSIONS

In this section, we will shed light on the properties of GHL shifts in details. For simplicity, we will find the following analytical solutions in the limit $\Delta = 0$ and discuss the negative and positive lateral shifts in cases of Klein tunneling and classical motion, respectively.

Case 1: Klein tunneling ($ss' = -1$). In this case, the critical angle (4) becomes

$$\phi'_c = \arcsin\left(\frac{V_0}{E} - 1\right), \quad (8)$$

when the condition $E < V_0 < 2E$ is satisfied. When the incidence angle ϕ_0 is less than the critical angle ϕ'_c obtained above, $\phi_0 < \phi'_c$, the lateral shift is given by

$$s_t = \frac{d \tan \phi_0}{f_0^2} \left\{ \left[2 + \left(\frac{k_0^2}{k_{x0}^2} + \frac{k_0^2}{q_{x0}^2} \right) \right] \frac{\sin(2q_{x0}d)}{2q_{x0}d} - \frac{k_0^2}{q_{x0}^2} \right\},$$

where $k_0 = (k_f k'_f + k_{y0}^2)^{1/2}$, and transmission probability T is given by Eq. (5),

$$T \equiv \frac{1}{f_0^2} = \left[\cos^2(q_{x0}d) + \frac{k_0^4}{k_{x0}^2 q_{x0}^2} \sin^2(q_{x0}d) \right]^{-1}. \quad (9)$$

The GHL shifts obtained above can be positive as well as negative, depending on the influence of $\sin(2q_{x0}d)/(2q_{x0}d)$. Since the inequality

$$\left[2 + \left(\frac{k_0^2}{k_{x0}^2} + \frac{k_0^2}{q_{x0}^2} \right) \right] > \frac{k_0^2}{q_{x0}^2}, \quad (10)$$

the lateral shifts can be positive only when $\sin(2q_{x0}d)/(2q_{x0}d) \rightarrow 1$ for a very thin barrier, namely $d \rightarrow 0$. However, the lateral shifts turn negative with increasing d . It is interesting that the negative lateral shifts can be enhanced by the transmission resonances. Since the transmission coefficient is an oscillating function of tunneling parameters and can exhibit any value from 0 to 1⁴, there are resonance conditions $q_{x0}d = N\pi$, $N = 0, \pm 1, \pm 2, \dots$ at which the barrier is transparent, $T = 1$. At resonances, the lateral shifts in this case reach $s|_{q_{x0}d=N\pi} = -(k_0^2/q_{x0}^2)d \tan \phi_0$, which correspond to the maximum absolute values. At anti-resonance, $q_{x0}d = (N + 1/2)\pi$, the lateral shifts becomes $s|_{q_{x0}d=(N+1/2)\pi} = -(k_{x0}^2/k_0^2)d \tan \phi_0$. The exotic behaviors of negative and positive GHL shifts are analogous to those of lateral shifts for the transmitted light beam through left-handed metamaterial slab¹⁴, based on the link between Klein paradox and negative refraction¹⁸.

On the contrary, when the incidence angle is larger than the critical angle ϕ'_c , $\phi_0 > \phi'_c$, the lateral shift becomes

$$s_t = \frac{d \tan \phi_0}{f_0^2} \left\{ \left[2 + \left(\frac{k_0^2}{\kappa_0^2} - \frac{k_0^2}{k_{x0}^2} \right) \right] \frac{\sinh(2\kappa_0 d)}{2\kappa_0 d} + \frac{k_0^2}{\kappa_0^2} \right\}.$$

In the limit of opaque barrier, $\kappa_0 d \rightarrow \infty$, the lateral shift trends to a constant as follows,

$$s_t = \frac{k_{y0}}{k_{x0} \kappa_0} \frac{2k_{x0}^2 \kappa_0^2 - k_0^2 (k_{x0}^2 - \kappa_0^2)}{k_{x0}^2 \kappa_0^2 + k_0^2}, \quad (11)$$

which is proportional to $1/\kappa_0$, and implies that the GHL shift in the evanescent case is in the same order of electron wavelength as the GH effect in a single graphene interface^{10,11}. More interestingly, the saturated GH shift is negative when the incidence angle satisfies $\phi'^c < \phi_0 < \phi^*$, where the critical angle is defined by

$$\phi^* = \arcsin \sqrt{\sin \phi'_c}. \quad (12)$$

But the GH shift in this case will become positive when $\phi_0 > \phi^*$. The sign change of GH shifts described by Fig. 3 (b) appears at the incidence angle $\phi_0 = \phi^*$, which is similar to the result of the quantum GH effect in graphene, taking the pseudospin degree into account¹¹.

Case 2: classical motion ($ss' = 1$). In this case, the critical angle is

$$\phi''_c = \arcsin\left(1 - \frac{V_0}{E}\right). \quad (13)$$

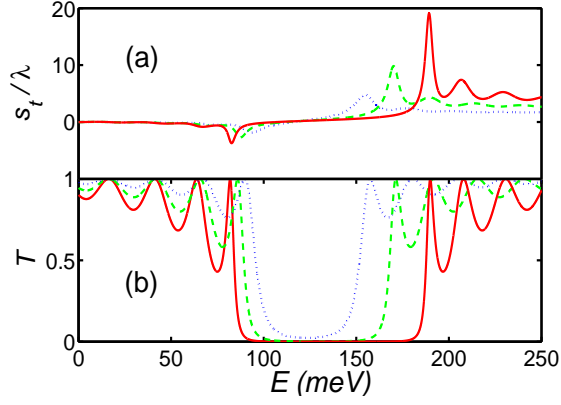


FIG. 4. (Color online) GHL shifts (a) and transmission gap (b) as the function of the incident energy E , where $d = 80\text{nm}$, $V_0 = 120\text{meV}$, and $\Delta = 0\text{meV}$. Solid, dashed, and dotted lines correspond to $\phi_0 = 20^\circ$, 15° , and 10° , respectively.

When the incidence angle is less than the critical angle for total reflection, $\phi_0 < \phi_c''$, the lateral shift can be written as

$$s_t = \frac{d \tan \phi_0}{f_0^2} \left\{ \frac{k_0'^2}{q_{x0}^2} + \left[2 - \left(\frac{k_0'^2}{k_{x0}^2} + \frac{k_0'^2}{q_{x0}^2} \right) \right] \frac{\sin(2q_{x0}d)}{2q_{x0}d} \right\},$$

where $k_0' = (k_f k_f' - k_{y0}^2)^{1/2}$, and transmission probability is

$$T \equiv \frac{1}{f_0^2} = \left[\cos^2(q_{x0}d) + \frac{k_0'^4}{k_{x0}^2 q_{x0}^2} \sin^2(q_{x0}d) \right]^{-1}, \quad (14)$$

Similarly, the lateral shifts for classical motion also depend periodically on the barrier's width, thus can be enhanced by the transmission resonances. The lateral shifts at resonances reach $s|_{q_{x0}d=N\pi} = (k_0'^2/q_{x0}^2)d \tan \phi_0$, while at anti-resonance they become $s|_{q_{x0}d=(N+1/2)\pi} = (k_{x0}^2/k_0'^2)d \tan \phi_0$. However, these GHL shifts in classical motion are always positive as those in the two-dimensional semiconductor barrier¹⁷. When $\phi_0 > \phi_c''$, the GHL shift in the evanescent case becomes

$$s_t = \frac{d \tan \phi_0}{f_0^2} \left\{ \frac{k_0'^2}{\kappa_0^2} + \left[2 - \left(\frac{k_0'^2}{\kappa_0^2} + \frac{k_0'^2}{k_{x0}^2} \right) \right] \frac{\sinh(2\kappa_0 d)}{2\kappa_0 d} \right\}.$$

Then the lateral shift in the limit, $\kappa_0 d \rightarrow \infty$, is given by

$$s_t = \frac{k_{y0}}{k_{x0}\kappa_0} \frac{2k_{x0}^2\kappa_0^2 + k_0'^2(k_{x0}^2 - \kappa_0^2)}{k_{x0}^2\kappa_0^2 + k_0'^2}, \quad (15)$$

which is always positive constant.

Based on the properties in two cases of Klein tunneling and classical motion, the GHL shifts (a) and corresponding transmission probabilities (b) as the function of incidence energy E are shown in Fig. 4, where $d = 80\text{nm}$, $V_0 = 120\text{meV}$, and $\Delta = 0\text{meV}$. Solid, dashed, and

dotted lines correspond to $\phi_0 = 20^\circ$, 15° , and 10° , respectively. It is shown that the GHL shifts is closely related to the transmission gap $\Delta E = 2\hbar k_y v_f$ ¹³. Fig. 4 indicates that the lateral shifts change the sign near the Dirac point $E = V_0$, and can also be enhanced by the transmission resonances near the boundaries of energy gap. In addition, the incidence angle has also great impact on the GHL shifts. The absolute values of the lateral shifts increase with increasing the incidence angles, and the positions of the maximum (absolute) values for the positive (negative) beam shifts can also be tuned because of the resonance conditions, as shown in Fig. 4.

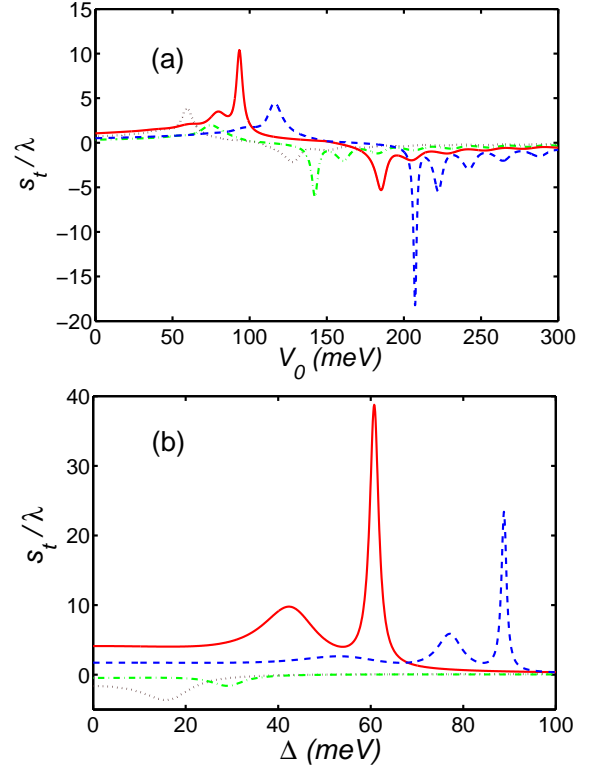


FIG. 5. (Color online) Dependence of GHL shifts on height V_0 of potential barrier (a) and induced gap Δ (b), where $d = 80\text{nm}$, (a) $\Delta = 0\text{meV}$, $E = 150\text{meV}$, $\phi_0 = 20^\circ$ (solid line), $E = 150\text{meV}$, $\phi_0 = 10^\circ$ (dashed line), $E = 100\text{meV}$, $\phi_0 = 20^\circ$ (dotted line), $E = 100\text{meV}$, $\phi_0 = 10^\circ$ (dot-dashed line); (b) $V_0 = 120\text{meV}$, $E = 220\text{meV}$, $\phi_0 = 20^\circ$ (solid line), $E = 220\text{meV}$, $\phi_0 = 10^\circ$ (dashed line), $E = 80\text{meV}$, $\phi_0 = 20^\circ$ (dotted line), $E = 80\text{meV}$, $\phi_0 = 10^\circ$ (dot-dashed line).

Finally, we will turn to discuss the modulations of GHL shifts by the height V_0 of potential barrier and the induced gap Δ . It is shown in Fig. 5 that the GHL shifts can be controlled by changing the height V_0 of potential barrier, which can be easily implemented by applying a local top gate voltage V_g to graphene¹⁶. Since the lateral shifts are in the forward and backward directions in

the cases of $E > V_0$ and $E < V_0$, respectively, it is suggested that the incidence energy can be selected by these tunable beam shifts. Thus, this phenomenon does result in an alternative way to realize the graphene-based electronic devices, for example, energy splitter and energy filter. Moreover, Fig. 5 (b) further investigate how the GH shifts are affected by a gap opening at the Dirac points. Comparisons of Figs. 2 and Figs. 3 further show that the energy gap will increase (decrease) the absolute values of the shifts in the propagating (evanescent) case. And the influence of gap in the propagating case is more pronounced than that in the evanescent one. The method to generate the energy gap in graphene is through an inversion symmetry breaking of the sublattice due to the fact the densities of the particles associated with the on-site energy for A and B sublattice are different⁵. Therefore, the periodical dependence of GH shifts on the gap provides an efficient way to modulate the lateral shifts in a fixed graphene barrier.

IV. CONCLUSION

In summary, we have investigated the GH shifts for Dirac fermions in transmission through a monolayer graphene barrier. The lateral shifts, as the functions of the barrier's width and the incidence angle, can be negative and positive in Klein tunneling and classical motion, respectively. Since the lateral shifts have a close rela-

tion with the transmission probability, the lateral shifts can be enhanced by the transmission resonances when the incidence angle is less than the critical angle for total reflection, while their magnitudes are only the order of Fermi wavelength when the incidence angle is larger than the critical angle. Compared with the smallness of conventional GH shift in graphene, the large negative and positive GH shifts, which can also be modulated by the height of potential barrier and the induced gap, will have potential applications in various graphene-based electronic devices. We further hope that these similar phenomena in magnetic graphene barrier may lead to the graphene-based spintronic devices on spin filter and spin beam splitter^{17,19}.

ACKNOWLEDGMENTS

This work is supported by the National Natural Science Foundation of China (Grants No. 60806041), the Shanghai Rising-Star Program (Grants No. 08QA14030), the Science and Technology Commission of Shanghai Municipal (Grants No. 08JC14097), the Shanghai Educational Development Foundation (Grants No. 2007CG52), and the Shanghai Leading Academic Discipline Program (Grants No. S30105). X. C. acknowledges Juan de la Cierva Programme of Spanish MICINN and FIS2009-12773-C02-01.

* xchen@shu.edu.cn

¹ A. H. Castro Neto, F. Guinea, N. M. R. Peres, K. S. Novoselov and A. K. Geim, *Rev. Mod. Phys.* **81**, 109 (2009).

² C. W. Beenakker, *Rev. Mod. Phys.* **80**, 1337 (2008).

³ K. S. Novoselov, A. K. Geim, S. V. Morozov, D. Jiang, Y. Zhang, S. V. Dubonos, I. V. Grigorieva, and A. A. Firsov, *Science* **306**, 666 (2004).

⁴ M. I. Katsnelson, K. S. Novoselov, and A. K. Geim, *Nat. Phys.* **2**, 620 (2006).

⁵ S. Y. Zhou, G. H. Gweon, A. V. Federov, P. N. First, W. A. de Heer, D. H. Lee, F. Guinea, A. H. Castro Neto, and A. Lanzara, *Nature Mater.* **6** 770 (2007).

⁶ V. V. Cheianov, V. Fal'ko, and B. L. Altshuler, *Science* **315**, 1252 (2007).

⁷ C. H. Park, Y. W. Son, L. Yang, M. L. Cohen, and S. G. Louie, *Nano Lett.* **8**, 2920 (2008).

⁸ P. Darancet, V. Olevano, and D. Mayou. *Phys. Rev. Lett.* **102**, 136803 (2009).

⁹ S. Ghosh, and M. Sharma, *J. Phys.: Condens. Matter*, **21**, 292204 (2009).

¹⁰ L. Zhao and S. F. Yelin, *Phys. Rev. B* **81**, 115441 (2010); arXiv:0804.2225v2.

¹¹ C. W. J. Beenakker, R. A. Sepkhanov, A. R. Akhmerov, and J. Tworzydło, *Phys. Rev. Lett.* **102**, 146804 (2009).

¹² K. L. Tsakmakidis, A. D. Boardman, and O. Hess, *Nature (London)* **450**, 397 (2007).

¹³ X. Chen and J.-W. Tao, *Appl. Phys. Lett.* **94**, 262102 (2009).

¹⁴ X. Chen and C. -F. Li, *Phys. Rev. E* **69**, 066617 (2004).

¹⁵ J.-H. Huang, Z.-L. Duan, H.-Y. Ling, and W.-P. Zhang, *Phys. Rev. A* **77**, 063608 (2008).

¹⁶ B. Huard, J. A. Sulpizio, N. Stander, K. Todd, B. Yang, and D. Goldhaber-Gordon, *Phys. Rev. Lett.* **98**, 236803 (2007).

¹⁷ X. Chen, C. -F. Li, and Y. Ban, *Phys. Rev. B* **77**, 073307 (2008).

¹⁸ D. Ö. Güney and D. A. Meyer, *Phys. Rev. A* **79**, 063834 (2009).

¹⁹ M. Sharma and S. Ghosh, arXiv: 0907.1631v1.